Paleotopographic and Depositional Environment Control on “Sweet Spot” Locations in Unconventional Resource Shales: Woodford and Barnett Shale Examples*

Roger M. Slatt[1], Brenton McCullough[1], Carlos Molinares[2], Elizabeth Baruch[1], Felipe Cardona[1], and Bryan Turner[1]

Search and Discovery Article #10713 (2015)**
Posted February 2, 2015

*Adapted from oral presentation given at Geoscience Technology Workshop, Expanding Unconventional Resources in Colombia with New Science - From Heavy Oil to Shale Gas/Shale Oil Opportunities, Bogota, Colombia, December 10-11, 2014

[1]Insitute of Reservoir Characterization, University of Oklahoma, Norman, Oklahoma (bryturner@gmail.com, rslatt@ou.edu)
[2]Conoco-Phillips Oil and Gas Co.

Abstract

Both the Woodford Shale (Oklahoma, U.S.A.) and the Barnett Shale (Texas, U.S.A.) are prolific unconventional resource shales. Both sit atop unconformities on the surface of underlying carbonate rocks. There is variable topographic relief on the unconformity surfaces due to incised valley and/or karst formation during periods of subaerial exposure resulting from lowered sea level. Anomalously high thicknesses of the shale can form within these topographic depressions, giving rise to potential “sweet spots” as drilling targets. Additionally, these shales often exhibit basal intervals of high gamma-ray log response, indicative of high organic matter (TOC). It is likely that the topographic relief that is formed during subaerial exposure creates areas of restricted marine circulation during early rise in sea level, and subsequent, localized anoxic depositional environments conducive to preservation of organic matter. It is possible that during the time after unconformity formation and prior to marine encroachment into incised valleys, lacustrine environments may form, which would be sites for earliest accumulation of organic-rich mud.

Selected References

Comer, J.B., 2008, Woodford Shale in southern Midcontinent, USA-Transgressive system tract marine source rocks on an arid passive continental margin with persistent oceanic upwelling: AAPG Annual Convention, San Antonio, TX, poster, 3 panels.

Grotzinger, J., and T.H. Jordan, 2010, Understanding Earth: W.H. Freeman, New York, 672 p.

Hester, T.C., J.W. Schmoker, and H.L. Sahl, 1990, Log-derived regional source-rock characteristics of the Woodford Shale, Anadarko basin, Oklahoma: U.S. Geological Survey Bulletin 1866-D, 38 p.

Jarvie, D.M., 2012, Shale resource systems for oil and gas: Part 1-Shale-gas resource systems: *in* J.A. Breyer, ed., Shale reservoirs—Giant resources for the 21st century: AAPG Memoir 97, p. 69–87.

Lambert, M.W., 1993, Internal stratigraphy and organic facies of the Devonian-Mississippian Chattanooga (Woodford) Shale in Oklahoma and Kansas, *in* B.J. Katz and L.M. Pratt, eds., Source rocks in a sequence stratigraphic framework: AAPG Studies in Geology 37, p. 163-176.

McCullough, B.J., and R.M. Slatt, 2014, Stratigraphic variability of the Woodford Shale across Oklahoma: AAPG Search and Discovery Article #80417, Website accessed January 23, 2015, http://www.searchanddiscovery.com/pdfz/documents/2014/80417mccullough/ndx_mccullough.pdf.html.

Paleotopographic and Depositional Environment Control on "Sweet Spot" Locations in Unconventional Resource Shales": Woodford and Barnett Shale Examples

Roger M. Slatt, Brenton McCullough, Carlos Molinares[1], Elizabeth Baruch, Felipe Cardona, and Bryan Turner*
Insitute of Reservoir Characterization, University of Oklahoma
1 Conoco-Phillips Oil and Gas. Co.

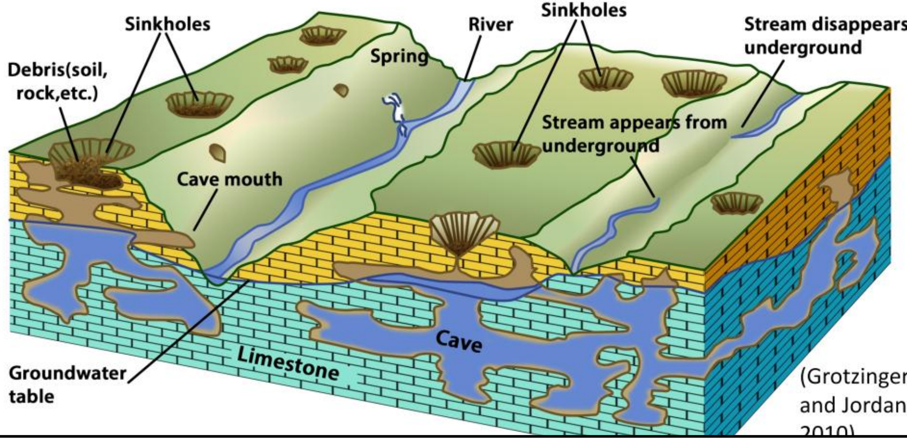

(Grotzinger and Jordan, 2010)

DEVONIAN-MISS. STRATIGRAPHIC COLUMN, OKLAHOMA

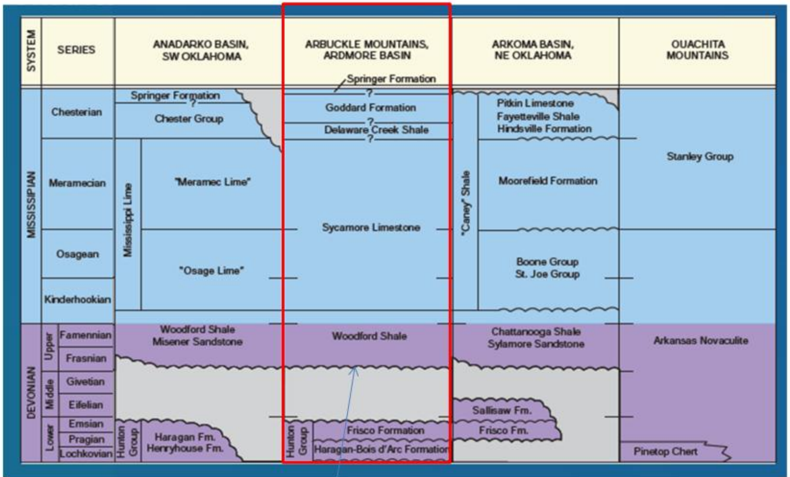

Major unconformity

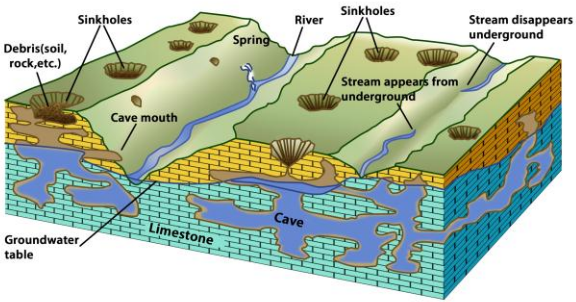

(Grotzinger and Jordan, 2010)

Seismically imaged Hunton surface

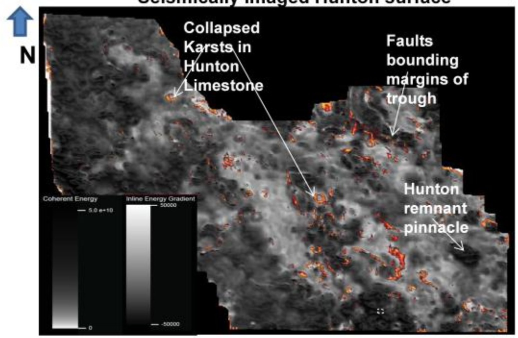

Althoff, Depositional megacycles in the Woodford Trough of central Oklahoma,
AAPG Woodford Forum, 4-12-2013

Woodford Incised valley fills and karst fills = potential sweet spots (greater thickness/organic-rich)

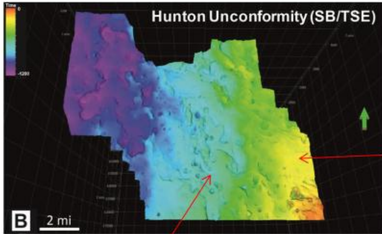

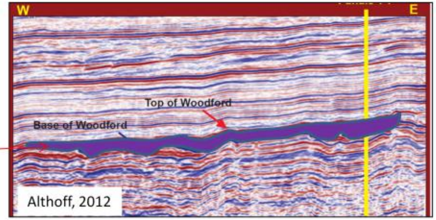

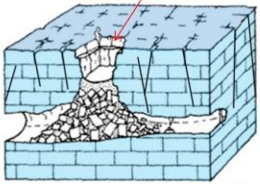

Karst

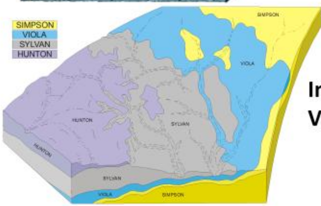

Incised Valley

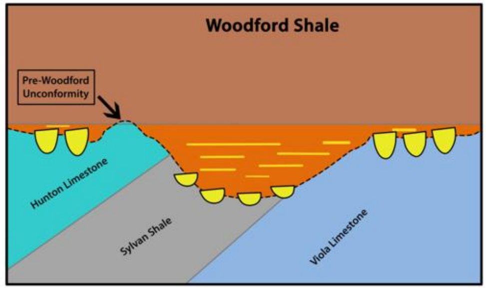

Dutton, T., Longfellow Energy LP, Emerging Shale Plays Conference – April 25, 2013

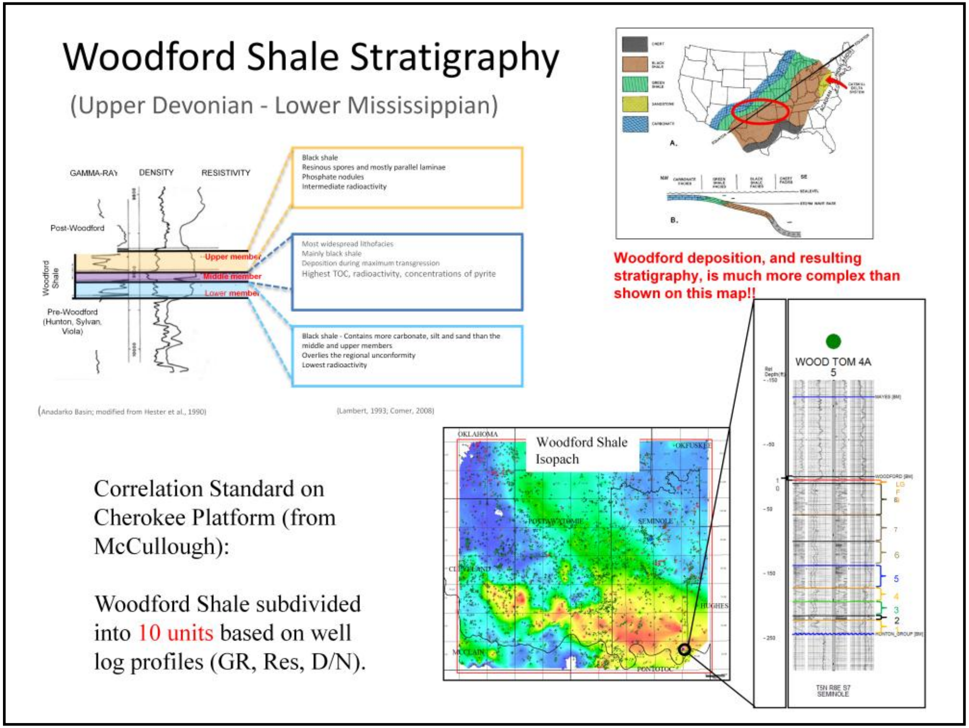

Presenter's notes:

- Organic rich black shale
- Thickness of the Woodford Shale ranges from 900 ft in the deep parts of the Anadarko Basin to 125 ft in the northern shelf
- In southern Oklahoma >700 ft, <200 ft
- Comer (2008) indicated that the thickness of the Woodford Shale is >500 ft in the Anadarko basin and <100 ft thick in the shelf areas and platforms

Woodford Incised Valleys

Valley fill is thin where underlying Hunton is thick and vice versa

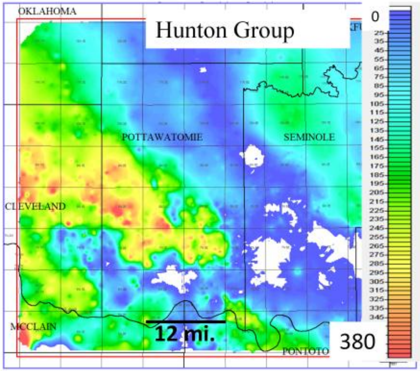

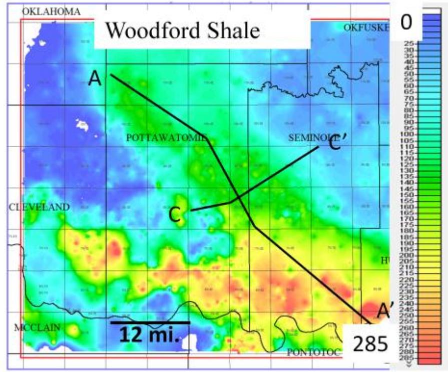

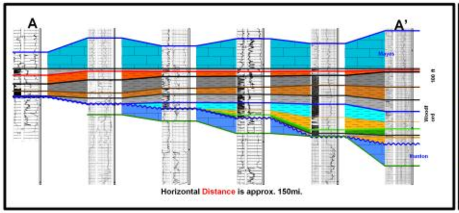

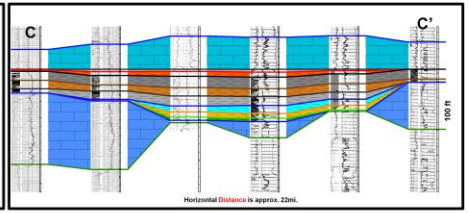

McCullough, 2014

The TOCpd for the top 10 shale-gas resource systems. Jarvie, 2012

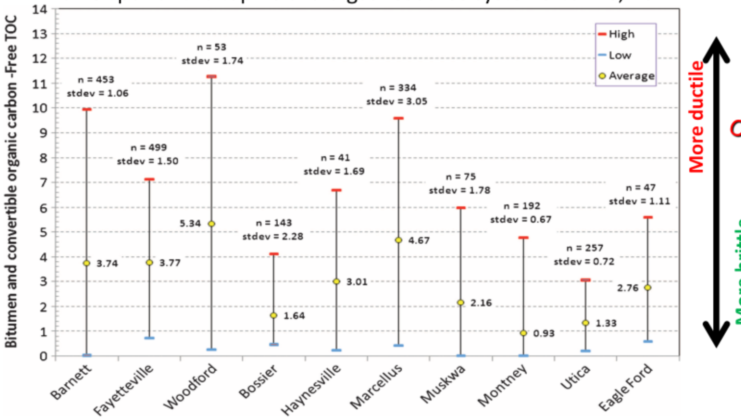

Organic matter quantity is determined by the total organic carbon (%TOC) content (whole-rock basis).

These data show the average TOCpd (present day) values for each system with the range of values, standard deviation, and number of samples. Given the high thermal maturity of these shales, these values are indicative of the nongenerative organic carbon (NGOC) values. TOCpd = present-day total organic carbon; stdev = standard deviation; n = number of samples.

Organic Geochemistry

Gamma-ray log of well W-2 showing the second-order sequence boundaries (SB) of the Woodford Shale and superimposed 3rd order parasequences.

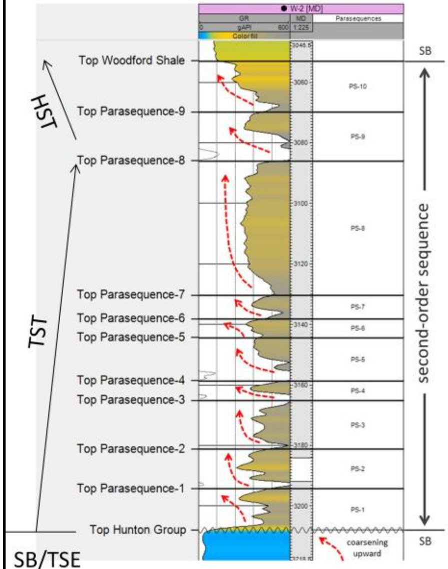

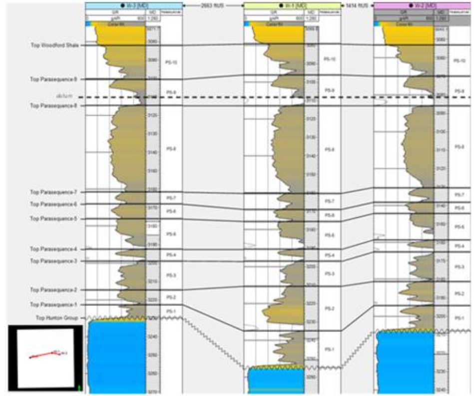

Cardona, 2014

TOC from seismic inversion of Woodford 3D seismic volume

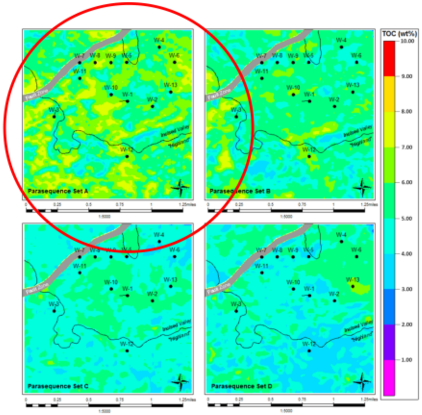

Total organic carbon (TOC) content maps for the Woodford Shale's parasequences sets in the study area. Dashed lines outline areas where this second-order sequence has more than 200 feet in thickness and are associated with pre-Woodford karsts or incised valleys

Vertical section through the TOC section and its correlation with the calculated log in the well W-3

Cardonas 2014

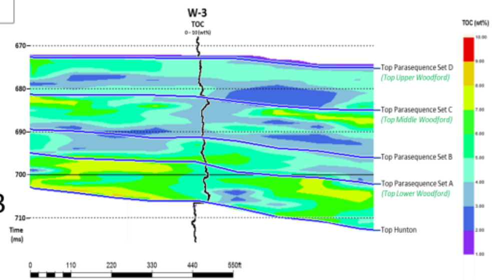

Cardona, 2014

Barnett Shale 3D horizon slices showing Karst surface and depressions into the overlying Barnett

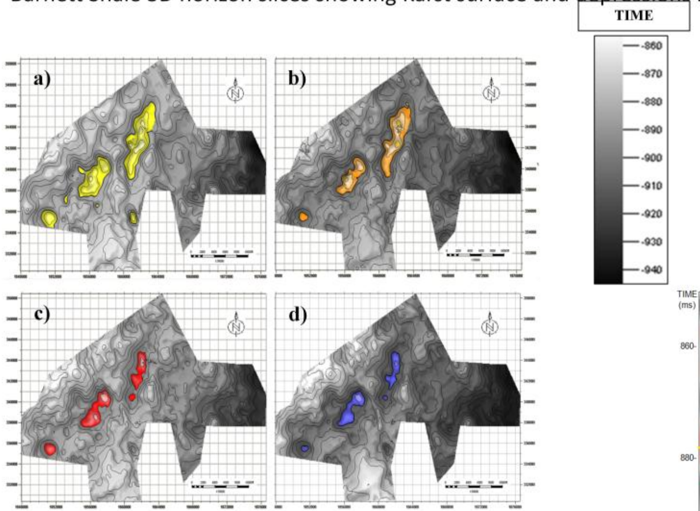

Areal distribution of karst topography on top of:
(a) GRPS 1,
(b) GRPS 2-3,
(c) Lower Barnett Sh,
(d) Upper Barnett Sh

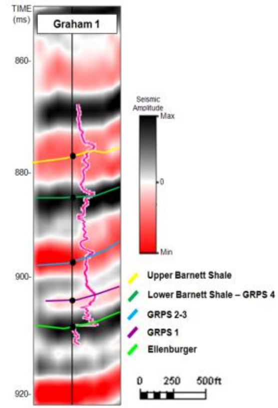

Baruch, 2011

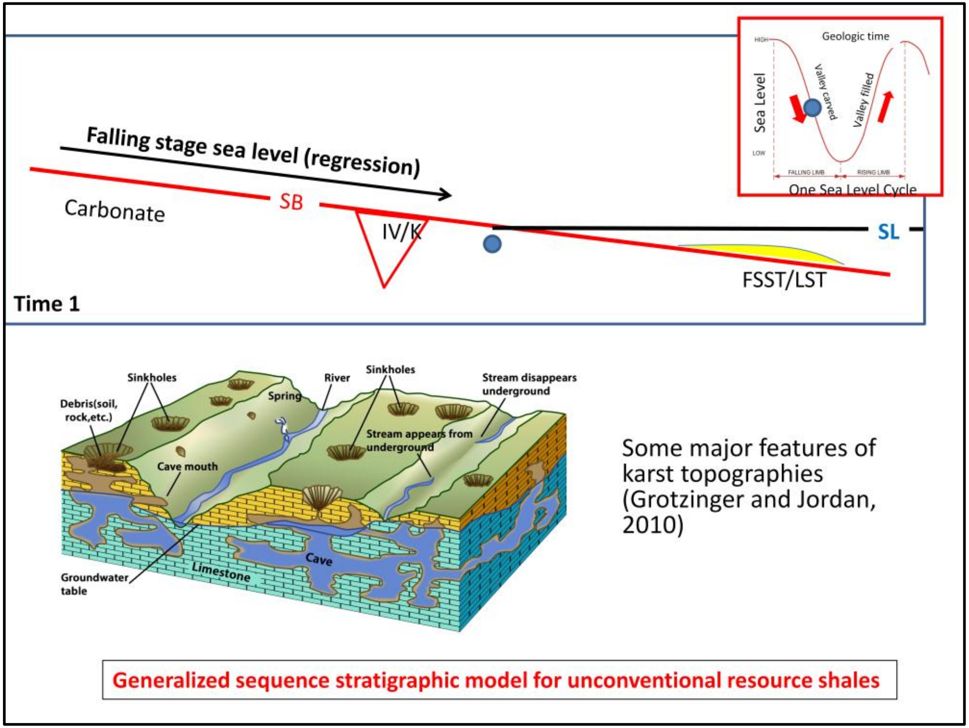

Presenter's notes: Generalized sequence stratigraphic model of unconventional resource shales. SB = Sequence Boundary; TSE = Transgressive Surface of Erosion; TST = Transgressive Systems Tract; CS = Condensed Section; mfs = maximum flooding surface; HST = Highstand Systems Tract. Two conceptual gamma ray logs are shown on the upper figure and on the lower left, to demonstrate the log responses of the different components. The lower middle diagram is a relative sea level curve illustrating the positions or times within a sea level cycle when each component is formed. The lower right diagram (after VanWagoner et al., 1990), shows 2^{nd} and 3^{rd} order cycles and a composite relative sea level curve of these two orders of cyclicity.

Time 2: Onset of Transgression

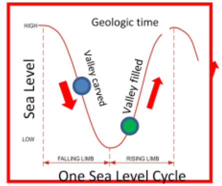

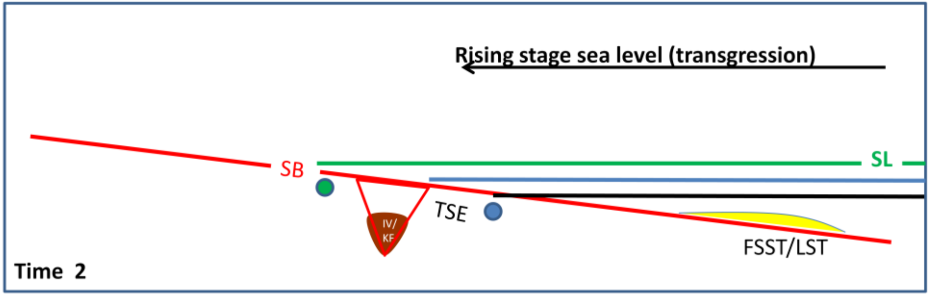

Generalized sequence stratigraphic model for unconventional resource shales

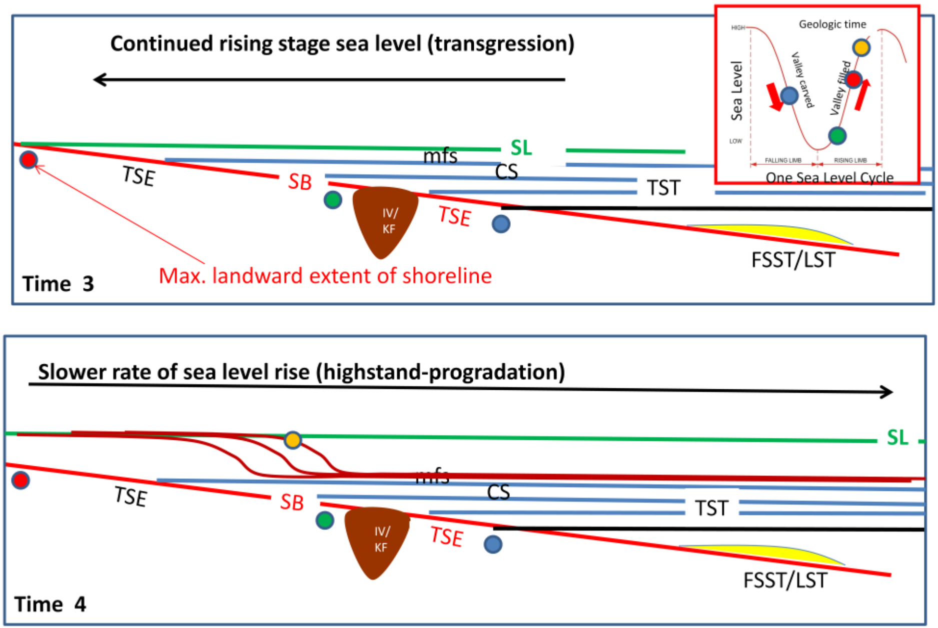

Generalized sequence stratigraphic model for unconventional resource shales

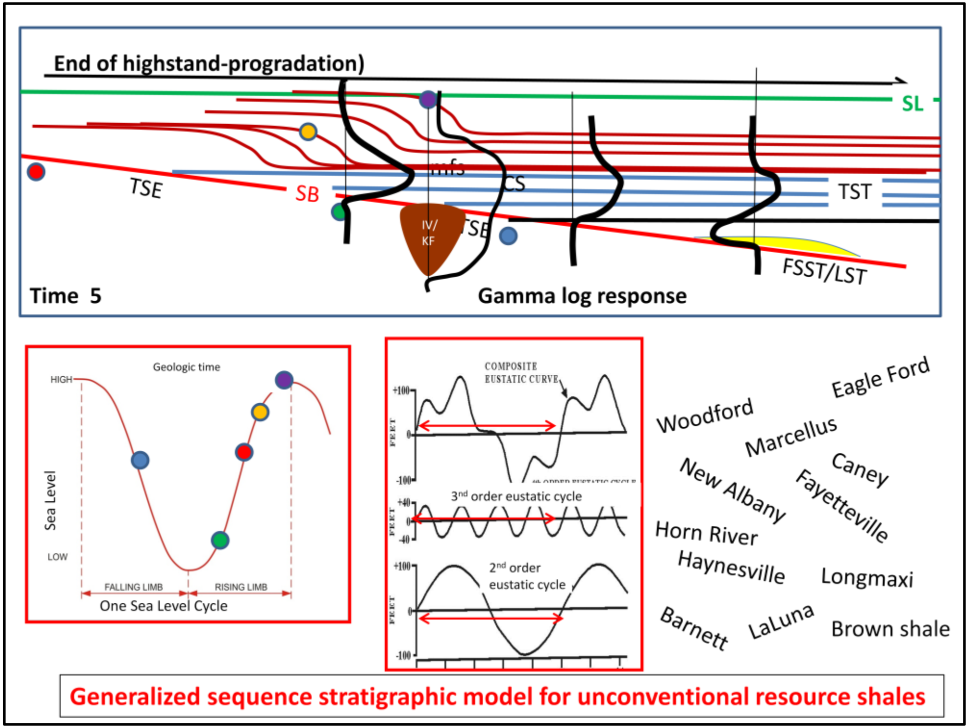

Presenter's notes: Generalized sequence stratigraphic model of unconventional resource shale as shown in five time steps (Time 1 to Time 5). SB = Sequence Boundary; FSST = Falling Stage Systems Tract; LST = Lowstand Systems Tract; TSE = Transgressive Surface of Erosion; TST = Transgressive Systems Tract; CS = Condensed Section; mfs = maximum flooding surface; HST = Highstand Systems Tract. The time steps are described in the text. A conceptual gamma ray log is shown on figure A both for stratigraphic sequences that formed landward of the minimum position of the shoreline (TST sits directly on SB/TSE) and seaward of the minimum position of the shoreline (FSST/LST sits below the TST). Figure B is a relative sea level curve illustrating the relative times within a sea level cycle when each component is formed. Figure C (after Van Wagoner et al., 1990) shows 2nd and 3rd order cycles and a composite relative sea level curve by superimposition of these two orders of cyclicity.